Difference correlation can distinguish deterministic chaos from $1/f^{\alpha}$-type colored noise

Tohru Ikeguchi
Department of Applied Electronics, Faculty of Industrial Science and Technology, Science University of Tokyo, 2641 Yamazaki, Noda-shi, Chiba 278, Japan

Kazuyuki Aihara
Department of Mathematical Engineering and Information Physics, Faculty of Engineering, The University of Tokyo, 7-3-1 Hongo, Bunkyo-ku, Tokyo 113, Japan

(Received 8 August 1996)

Distinguishing deterministic chaos from colored noise with the power-law spectra or random fractal sequences (fractional Brownian motions) is one of the important problems in chaotic time series analysis. In this paper, we describe a simple method for solving this problem, which seems easier than the other algorithms that have already been proposed. In order to show how well our procedure works, first we apply a nonlinear prediction to time series data, produced from both nonlinear dynamical systems and stochastic systems with the power-law spectra. Next, we evaluate the prediction performance by calculating two kinds of correlation coefficients between actual time series and predicted time series, which are called a conventional correlation coefficient and a difference correlation coefficient. The conventional correlation coefficient is a usual correlation coefficient between actual time series and predicted time series, and the difference correlation coefficient is between first-difference time series obtained from actual time series and predicted time series. When the one-step-ahead nonlinear prediction is applied to deterministic chaos without observational noise, not only conventional correlation coefficients but also difference correlation coefficients are very high values, namely, the coefficients take values almost 1.0 even if the number of data points is small. On the other hand, in the case of $1/f^{\alpha}$-type colored noise, although conventional correlation coefficients are relatively high values, difference correlation coefficients turn out to be low values, even though the scaling exponent of the power spectrum α is large. This difference between conventional correlation and difference correlation can be a good criterion for distinguishing deterministic chaos from colored noise with the power-law spectra. Finally, several real time series data are analyzed in order to confirm the applicability of the proposed method.
[S1063-651X(97)10403-2]

PACS number(s): 05.45.+b, 02.60.−x

I. INTRODUCTION

The identification of deterministic chaos and reconstruction of its dynamics are important research topics from the viewpoint of chaotic time series analysis. For this purpose, the estimation of correlation dimensions of underlying possible attractors has been playing a central role; however, there are several drawbacks in its application to real time series data. For example, the number of points for calculating dimensions should be large enough to obtain reliable results. Moreover, estimating such dimensions usually requires one to extract a scaling exponent. This step of extracting the scaling region is sometimes dangerous, or at least unreliable, because it can include an arbitrary choice for determining scaling regions.

Next, attention has been moved to Lyapunov spectral analysis, which gives us important information on orbital instabilities peculiar to chaotic dynamics. However, there are also several drawbacks with this analysis. For example, if an algorithm for estimating Lyapunov spectra is blindly applied to a time series that has a stochastic origin, it has been shown that spurious positive Lyapunov exponents would be obtained [1,2].

Recently, nonlinear prediction has shown the ability to distinguish deterministic chaos from randomness and noisy periodicity [3]. It was shown that prediction performance against prediction steps should decrease because of orbital instability peculiar to chaotic dynamics. However, if the time series is a realization of the random process, the prediction performance is always bad and then it takes a value nearly zero against any prediction step. When the time series is periodic, it is fundamentally possible to predict in any prediction step and then the prediction performance versus the prediction step is almost flat.

Wales has shown that one can estimate the largest positive Lyapunov exponent by calculating the loss of information or the slope of the decreasing property [4]. The results in Ref. [3] also imply the sensitivity of prediction performance on the dimensions of reconstructed attractors and therefore one can find an optimal reconstructing dimension.

However, if the observed time series is produced from stochastic systems with the power-law spectra, or $1/f^{\alpha}$, there is the same tendency that prediction performances decrease with increasing prediction steps, which is the same with deterministic chaos. Therefore, one cannot distinguish deterministic chaos from colored noise with the power-law spectra if one extracts only the decreasing properties of prediction performance against prediction steps. This problem is important because deterministic dynamical systems can generate the power-law spectra and, on the other hand, there are also many natural stochastic phenomena that exhibit the power-law spectra.

Tsonis and Elsner showed how to distinguish deterministic chaos from this kind of colored noise or random fractal sequences (fractional Brownian motion) [5]. They describe that the semi-log and the log-log plots of the relation between the prediction steps and the correlation coefficients between actual time series and predicted time series show different properties if the prediction algorithm is applied to these time series. If the time series is produced from deterministic dynamical systems, the correlation coefficients should decrease exponentially with prediction steps. In the case of colored noise that has the power-law spectrum of the form $1/f^{\alpha}$ or a random fractal sequence, the prediction accuracy is linearly decreasing in the log-log plots. Therefore, if one plots the prediction performance with the semi-log and the log-log plots, these two time series can be distinguished, because they show different properties.

Although their approach is promising on distinguishing chaos from colored noise with the power-law spectra or random fractal sequences, as Tsonis and Elesner have indicated [5] that it may be difficult to extract the scaling law in the case of analyzing real time series data because real time series data are usually corrupted by noise, the number of data points is limited, and the resolution of the data is finite. From the viewpoint of real time series analysis, it is important to clarify the limitation of the algorithms for discriminating noisy chaotic dynamics from $1/f^{\alpha}$-type colored noise.

In this paper, we propose another method with the ''difference correlation'' to distinguish deterministic chaos from $1/f^{\alpha}$-type colored noise or random fractal sequences. Here, by the term of the difference correlation we mean the correlation coefficients between two time series, namely, the first-difference time series obtained from actual time series and predicted time series [6].

In the following, first we apply nonlinear prediction to deterministic chaos and colored noise or random fractal sequences and show the efficiency of discrimination by calculating both the conventional and the difference correlation coefficients. Second, we analyze the prediction performance in the case of noisy chaos in order to clarify the limit on the discrimination of deterministic chaos with noise from $1/f^{\alpha}$ type colored noise. Finally, we show several results obtained from the analysis with our proposed method on real time series data from real world systems.

II. NONLINEAR PREDICTION AS A WAY OF DISTINGUISHING DETERMINISTIC CHAOS FROM COLORED NOISE WITH THE POWER-LAW SPECTRA

In this section, we make two kinds of time series: the first is produced by deterministic dynamical systems and the second is colored noise with the power-law spectra or random fractal sequences. As examples of deterministic chaos we use the Hénon map [7], the Ikeda map [8], and the Bernoulli map [9]. The Hénon map [7] is described by the equations

$$x_1(t+1)=1+x_2(t)-ax_1(t)^2,$$
$$x_2(t+1)=bx_1(t), \tag{2.1}$$

where a and b are the parameters and fixed at 1.4 and 0.3, respectively. The second example is the Ikeda map [8], which is described by the equations

$$x_1(t+1)=q+b[x_1(t)\cos\theta(t)-x_2(t)\sin\theta(t)],$$
$$x_2(t+1)=b[x_2(t)\sin\theta(t)+x_2(t)\sin\theta(t)], \tag{2.2}$$

where $\theta(t)=\kappa-\alpha/[1+x_1(t)^2+x_2(t)^2]$ and the values of q, κ, α, and b are fixed at 1.0, 0.4, 6.0, and 0.7, respectively. The third example is the Bernoulli map [9], described as

$$x(t+1)=\begin{cases} x(t)+2^{B-1}(1-2\epsilon)x(t)^B+\epsilon, & 0\leqslant x(t)\leqslant\frac{1}{2} \\ x(t)-2^{B-1}(1-2\epsilon)[1-x(t)^B]-\epsilon, & \frac{1}{2}\leqslant x(t)\leqslant 1, \end{cases} \tag{2.3}$$

where the values of B and ϵ are fixed at 2.0 and 10^{-13}, respectively.

The reason why these dynamical systems are adopted is that these examples have different characteristics on their power spectra. Figure 1 shows the power spectra calculated for the dynamical systems described above. While the characteristics of power spectra of the Hénon map and the Ikeda map are almost similar, for the Bernoulli map, the power spectrum has the $1/f^{\alpha}$-type form. Although there are several dynamical systems with $1/f^{\alpha}$-type spectra, for instance, as indicated in Ref. [10], they are not considered to be ''low-dimensional'' dynamical systems. Therefore, we use the Bernoulli map as an example of a deterministic system that has the power-law spectrum [9].

Next we numerically produce $1/f^{\alpha}$-type colored noise or random fractal sequences. A random fractal sequence or a fractional Brownian motion is a realization of stochastic process, which has the property that the power spectrum $P(f)$ has the form of $P(f)\propto 1/f^{\alpha}$, where α is a constant. In order to produce the time series with the power spectrum of the above form, first, we decide the sampling rate, the number of data points, and the value of the scaling parameter α and generate a power spectrum with a form of $1/f^{\alpha}$. Then, phases of the power spectrum are randomized by pseudorandom numbers uniformly distributed on $[0,2\pi]$. Finally, applying the inverse Fourier transform to this phase-randomized power spectrum, we obtain the time series that has the $1/f^{\alpha}$ power spectrum with arbitrary values of α [11]. For example, Brownian motions are the case with $\alpha=2$. Any time series with a $1/f^{\alpha}$ property with arbitrary α can also be obtained by integrating the realization of Brownian motions

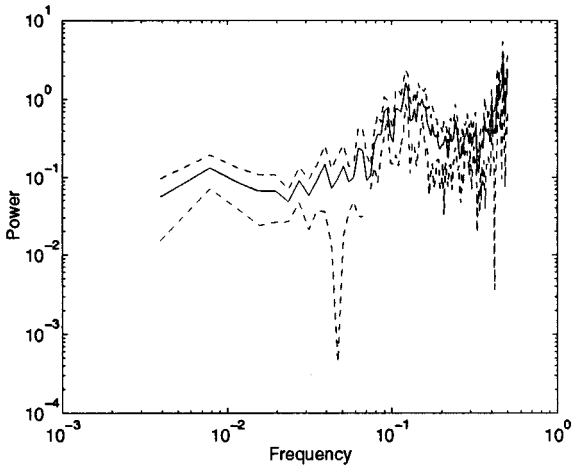

(a) the Hénon map

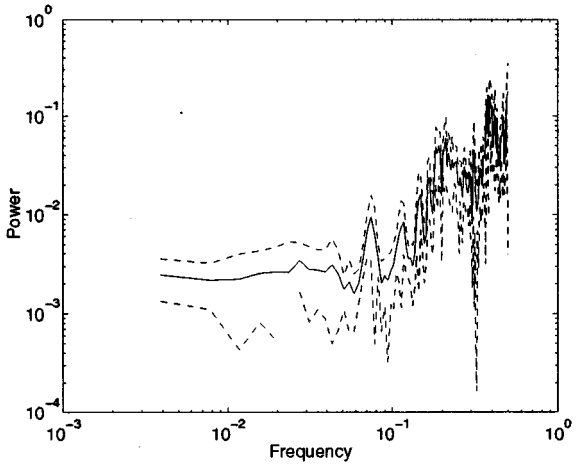

(b) the Ikeda map

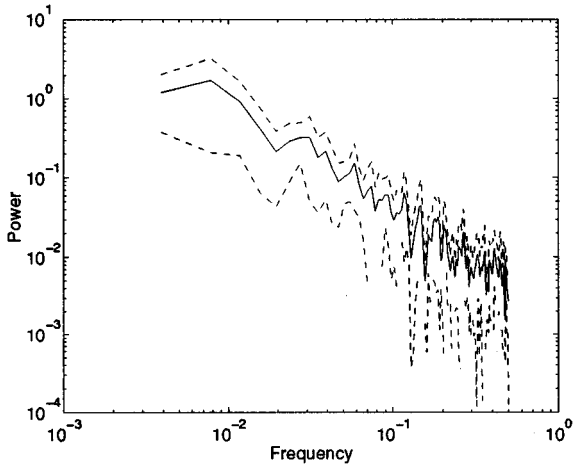

(c) the Bernoulli map

FIG. 1. Examples of power spectra obtained from the dynamical systems described in the text: (a) The Hénon map, (b) the Ikeda map, and (c) the Bernoulli map. The number of data points for calculating Fourier transforms is 256 with the Hanning window. Dashed lines represent 95% confidence intervals.

with fractional times. This is why the time series is called a fractional Brownian motion or a random fractal sequence.

As a nonlinear prediction algorithm, we use a kind of local linear approximation, which we call a modified version of the method of analogues [12] and has high performance even if the observed time series are contaminated by additive uncorrelated noise [6]. Let us consider the state space in which the trajectory of the attractor is reconstructed and a point, whose future behavior will be predicted, denoted by $\boldsymbol{v}_T$. A set of neighbors of the point $\boldsymbol{v}_T$, which are designated by $\boldsymbol{v}_{k_i}$ $(i=1,2,\ldots,M)$, are searched from all points on the reconstructed attractor. The selected neighbors are sorted in ascending order, namely, $\boldsymbol{v}_{k_1}$ is the nearest neighbor of $\boldsymbol{v}_T$ and so on. After p time steps, $\boldsymbol{v}_{k_1}$ is mapped to $\boldsymbol{v}_{k_1+p}$.

Then we estimate $\hat{\boldsymbol{v}}_{T+p}$ by

$$\hat{\boldsymbol{v}}_{T+p}=\sum_{i=1}^{M} \boldsymbol{w}(\boldsymbol{v}_{k_i},\boldsymbol{v}_T)\boldsymbol{v}_{k_i+p}, \tag{2.4}$$

where $\boldsymbol{w}(\ )$ is a weighting function depending only on the distance between $\boldsymbol{v}_T$ and $\boldsymbol{v}_{k_i}$. For the sake of simplicity, we use a simple form of the weighting function, that is, the explicit form of the prediction algorithm is described by

$$\hat{\boldsymbol{v}}_{T+p}=\frac{\sum_{i=1}^{M} \frac{1}{|\boldsymbol{v}_{k_i}-\boldsymbol{v}_T|}\boldsymbol{v}_{k_i+p}}{\sum_{i=1}^{M} \frac{1}{|\boldsymbol{v}_{k_i}-\boldsymbol{v}_T|}}. \tag{2.5}$$

In applying this algorithm to real time series, singular cases with $\boldsymbol{v}_T=\boldsymbol{v}_{k_i}$ due to, e.g., observational noise and finite resolution of data, can be avoided by introducing an exceptional rule that if $\boldsymbol{v}_T=\boldsymbol{v}_{k_1}$, then $\hat{\boldsymbol{v}}_{T+p}=\boldsymbol{v}_{k_1+p}$.

For evaluating prediction performance, here we use two measures that relate predicted time series to actual time series. The first is the correlation coefficient r_1 defined as

$$r_1=\frac{\sum_{i=1}^{P}[z(t)-\overline{z}][\hat{z}(t)-\overline{\hat{z}}]}{\sqrt{\sum_{i=1}^{P}[z(t)-\overline{z}]^2}\sqrt{\sum_{i=1}^{P}[\hat{z}(t)-\overline{\hat{z}}]^2}}, \tag{2.6}$$

where $z(t)$ and $\hat{z}(t)$ are actual and predicted time series, $\overline{z}$ and $\overline{\hat{z}}$ are the averages, and P is the number of data points in the predicted time series.

The second is the correlation coefficient r_2 between the first-difference time series $\Delta z(t)=z(t+1)-z(t)$ and $\Delta\hat{z}(t)=\hat{z}(t+1)-z(t)$,

$$r_2=\frac{\sum_{i=1}^{P'}[\Delta z(t)-\Delta\overline{z}][\Delta\hat{z}(t)-\Delta\overline{\hat{z}}]}{\sqrt{\sum_{i=1}^{P'}[\Delta z(t)-\Delta\overline{z}]^2}\sqrt{\sum_{i=1}^{P'}[\Delta\hat{z}(t)-\Delta\overline{\hat{z}}]^2}}, \tag{2.7}$$

where P' is the number of data points in the time series $\Delta\hat{z}(t)$. While the former coefficient r_1 is called the conventional correlation coefficient, the latter coefficient is called the difference correlation coefficient; for distinguishing deterministic chaos from colored noise with the power-law

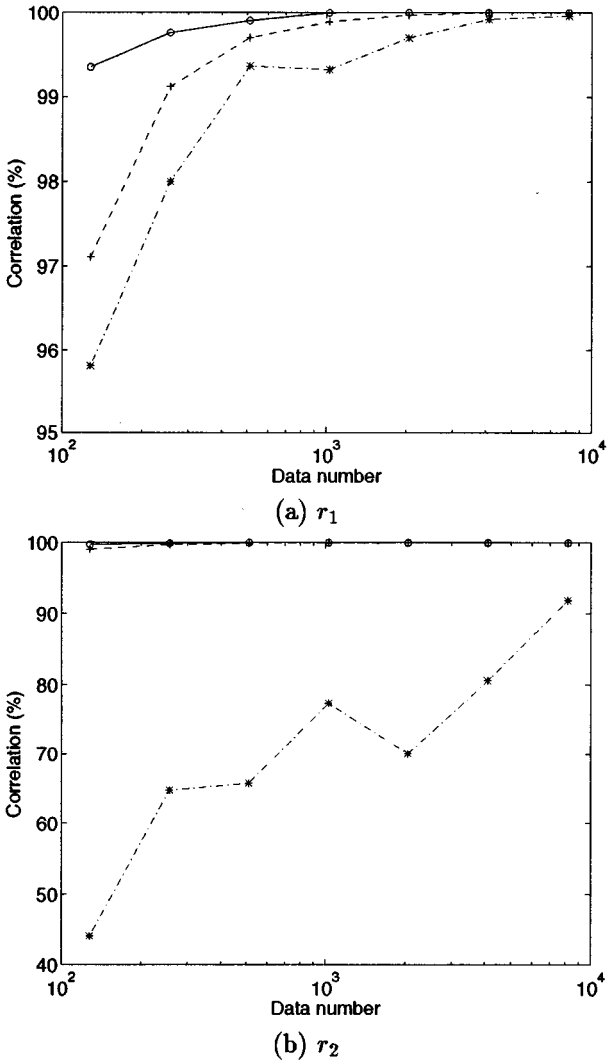

FIG. 2. Relation between correlation coefficients and the number of data points in a time series in the case that time series are produced from deterministic chaos. The prediction step is fixed to one. The result of r_1 is shown in (a) and r_2 in (b). In these figures, attractors are reconstructed in two-, three-, and two-dimensional state spaces, for the Hénon map (solid lines with circles), the Ikeda map (dashed lines with pluses) and the Bernoulli map (dotted dashed lines with asterisks), respectively. The value of lag is fixed at 1 in each case. The estimated values of r_1 and r_2 are obtained by averaging over 100 trials.

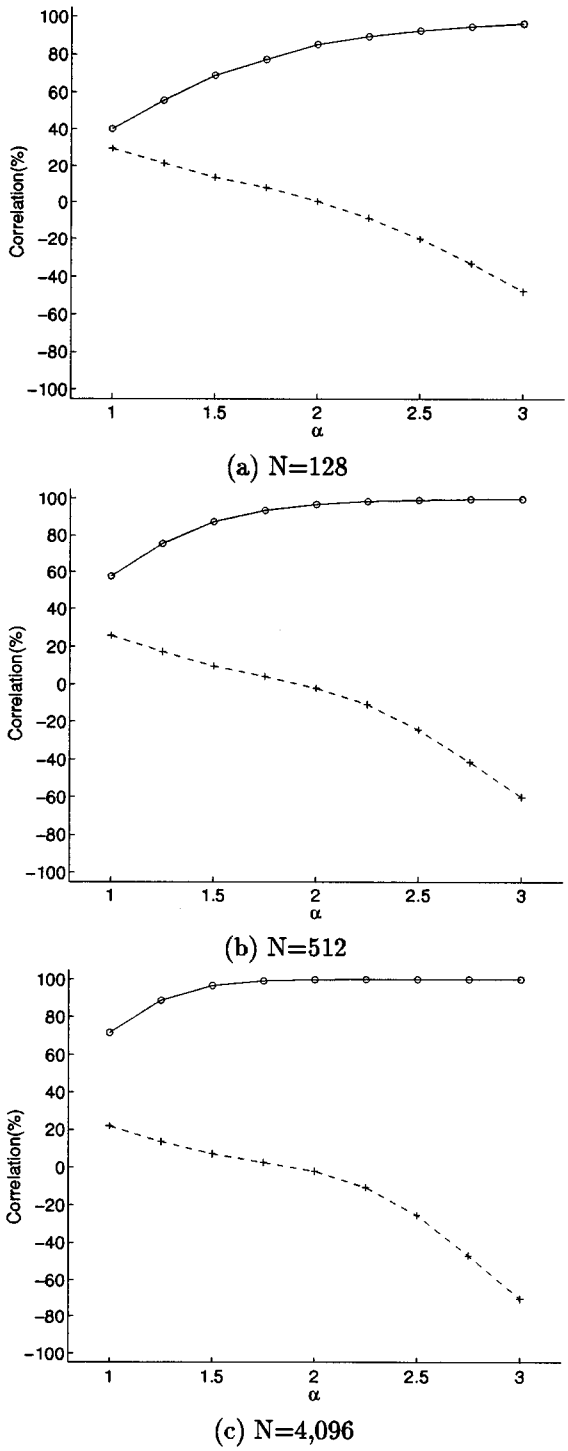

FIG. 3. Prediction performance evaluated on colored noise. The numbers of data points N are (a) 128, (b) 512, and (c) 4096. The abscissa is the scaling parameter α and the ordinate is the correlation coefficients. Both conventional and difference correlation coefficients are plotted in the same figure. Solid lines with circles indicate the conventional correlation coefficients and dashed lines with pluses the difference correlation coefficients. These correlation coefficients are the averaged value with 1000 trials.

spectra, the latter quantity, or the difference correlation coefficient r_2, plays a very important role.

Figure 2 shows the prediction performances calculated on dynamical systems. This is the plots of r_1 and r_2 with varying the number of data points for making a database of prediction in the case of the one-step-ahead prediction. The first half of the time series is used for making a database, and nonlinear prediction is applied to the second half in order to evaluate the prediction performance. Therefore, the two correlation coefficients are calculated with the second halves.

Here we should mention that for the Hénon map and the Ikeda map, the prediction performances are good for almost all trials with different initial conditions for producing time series. For the Bernoulli map, since the response exhibits intermittency, sometimes the prediction performance is worse, especially for a smaller number of data points. This is because when the number of data points is small, it happens that the first half time series for making a database includes only the laminar phase or the bursting phase. Therefore, the

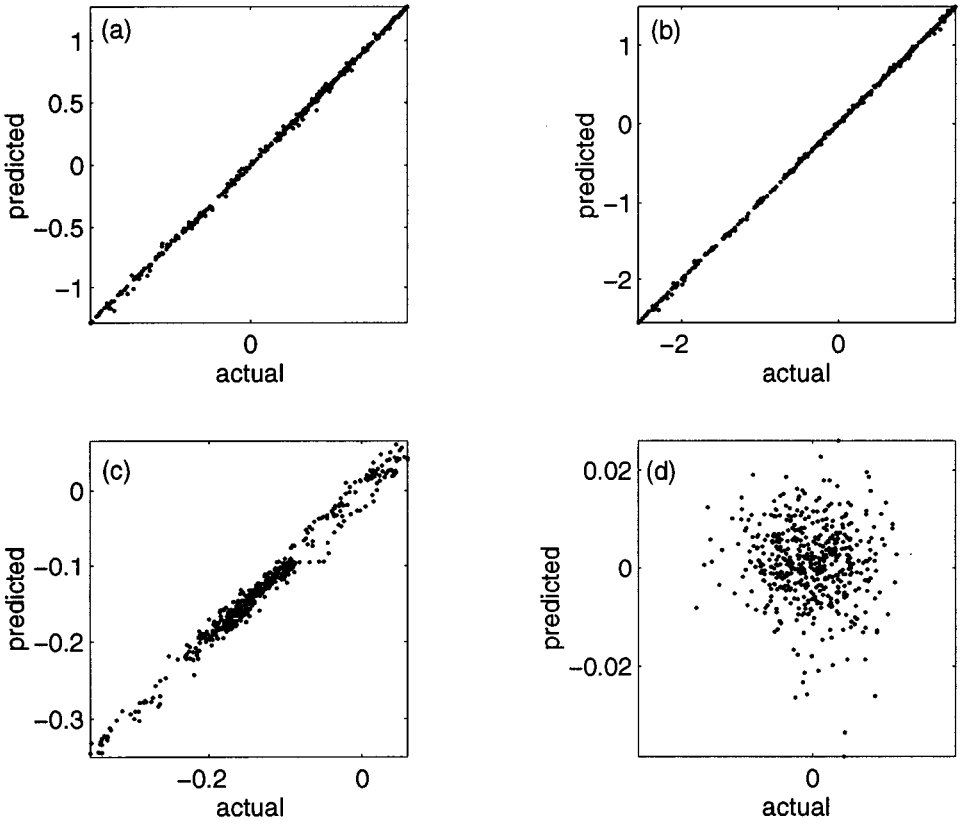

FIG. 4. Examples of correlation plots for the dynamical system and colored noise. Plotted in (a) are $z(t)$ and $\hat{z}(t)$ of the Hénon map, and in (b) $\Delta z(t)$ and $\Delta\hat{z}(t)$ of the Hénon map. The reconstructed dimension is 2. Shown in (c) and (d) are the corresponding correlation plots for colored noise with $\alpha=2.0$. The reconstructed dimension is 3. The abscissas are actual values and the ordinates are predicted values.

prediction performance gets worse for fewer data points. However, if the observed time series includes enough points, namely, both the laminar phase and the bursting phase, the prediction efficiency would be good for the one-step-ahead prediction.

In conclusion, in any cases where these examples of deterministic chaos are analyzed, not only the conventional correlation coefficients, but also the difference correlation coefficients show high values for the short-term prediction [3] because the assumption of the existence of deterministic dynamics is appropriate and the algorithm of nonlinear prediction is suitable for extracting the deterministic dynamics from the time series.

Figure 3 shows the results of an application of the nonlinear prediction to colored noise with the power-law spectra. The values of the scaling parameter α for $1/f^{\alpha}$ noise are varied from 1.0 to 3.0 with the regular interval $\Delta\alpha=0.25$. In Fig. 3, the prediction step is fixed to one. From this result, we can read the two tendencies.

Even though α is small, the conventional correlation coefficients exhibit relatively higher values. When α increases from 1.0 to 3.0, the conventional correlation coefficient converges to nearly 100%. The property of exhibiting high values of the conventional correlation coefficients in a short-term prediction is the same characteristic as for deterministic chaos. If we calculate only this quantity, there is a possibility that colored noise with the power-law spectrum might be misinterpreted as deterministic chaos.

However, the difference correlation coefficients show a different property. Namely, they are not as high as the conventional correlation coefficients, even when α is large. Here we recall that for deterministic chaos, not only conventional correlation coefficients, but also difference correlation coefficients take high values (see Fig. 2).

In Fig. 4, correlation plots are shown for the Hénon map and $1/f^2$ colored noise. Figure 5 shows the same results as in Fig. 4, but they are represented as a time series. From these figures, we obtain more strong evidence that there are different properties between deterministic chaos and $1/f^{\alpha}$-type colored noise.

In the case of deterministic chaos, we can see that actual and predicted values are almost distributed on the diagonal lines as shown in Figs. 4(a) and 4(b). However, in the case of colored noise with the power-law spectra, although actual and predicted values used for the conventional correlation coefficient are almost on the diagonal line [Fig. 4(c)], for the first-difference data of Fig. 4(d) they seem to be distributed almost randomly. This tendency is also confirmed in Fig. 5. In Figs. 5(a) and 5(b), actual and predicted time series are plotted with time step t. In the case of the deterministic chaos, since the assumption of the existence of deterministic dynamics is appropriate, predicted points are almost the same as actual points; therefore it is impossible to distinguish solid and dashed lines. But in Figs. 5(c) and 5(d), although the slow trends of both actual and predicted times series look similar [Fig. 5(c)], if the fine structures of movements are observed, we can realize that the predicted time series just follow the actual time series after a one step [Fig. 5(d)]. This is why the conventional correlation coefficients exhibit high performances and the difference correlation coefficients are worse.

In conclusion, these properties on colored noise are different from the results of deterministic chaos; this shows that colored noise with the power-law spectra can be distin-

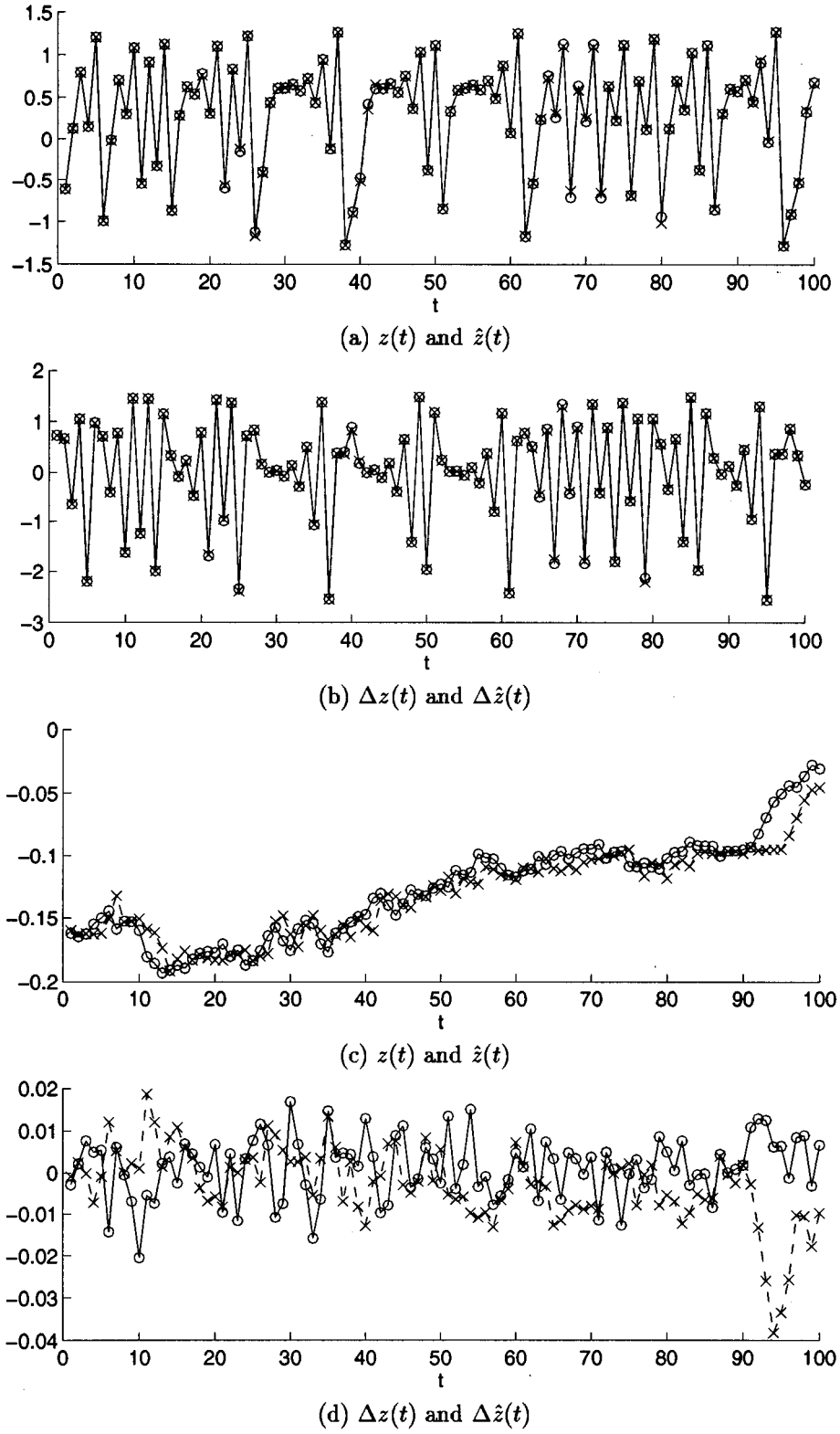

FIG. 5. Same as Fig. 4, but represented as the time series. (a) and (b) are for the Hénon map and (c) and (d) are for colored noise. Solid lines with circles are actual values and dashed lines with crosses predicted values.

guished from deterministic chaos if nonlinear prediction is applied and the two evaluation criteria, namely, both the conventional and the difference correlation coefficients, are computed. It should be noted that the results we show in this section are obtained only with a one-step-ahead prediction; this implies that we need not necessarily calculate prediction performance in various prediction steps as for extracting the scaling laws with the semi-log and the log-log plots.

III. LIMITS ON DISCRIMINATING NOISY CHAOS FROM COLORED NOISE WITH THE POWER-LAW SPECTRA

In the preceding section, we have shown that the difference correlation coefficient can be a good measure for distinguishing deterministic chaos from colored noise with the power-law spectra. However, observational noise is not con-

sidered because it is necessary to clarify the discrimination power under an idealized condition before applying to real data.

For real time series, on the other hand, corruption by observational noise is unavoidable; therefore, the performance of discrimination of noisy chaos from colored noise with the power-law spectra is also important from the viewpoint of handling real data. We should recognize that if a large amount of stochastic noise is added to chaotic time series, namely, the variance of the noise is relatively larger than that of the chaotic time series, it is very difficult to distinguish deterministic chaos from stochastic noise especially when the amount of information on the observable is limited; for example, the number of data points is limited and the resolution of each data is finite. This is always the case for analyzing real data.

Therefore, in this section, we analyze the prediction performance of noisy chaos and discrimination characteristics and discuss where the limit is on the discrimination of noisy deterministic chaos from stochastic time series with the power-law spectra.

Figure 6 shows the prediction performance when random noise with several levels is added to the dynamical systems. In the figure, the prediction step is fixed to 1. The abscissa shows the noise levels measured in the signal-to-noise ratio and the ordinate the correlation coefficients. The value of 0 dB in the signal-to-noise ratio means that the total variances of time series and additive random noise are the same level.

From this result, even if the signal-to-noise ratio is 10 dB, in which the original time series is heavily contaminated with additive random noise, it is possibile to distinguish deterministic chaos from colored noise by the conventional correlation and the difference correlation coefficients, at least for the Hénon map and the Ikeda map. If we can obtain a cleaner and longer time series, it is possible that the discriminant strategy of computing both the conventional and difference correlation coefficients is more effective.

IV. APPLICATION OF THE ALGORITHM TO REAL TIME SERIES

In this section, we will show several results from analyzing real time series with the proposed discrimination method. The first example of real time series is data on squid giant axon response to periodic pulses, which have already been reported to exhibit chaotic behavior with various analyses [13,14], including nonlinear prediction [15]. This time series can be a good example of a real time series that exhibits chaotic behavior.

The second example is Lorenz-like chaos in a NH_3–far infrared (FIR) laser, which has been prepared as one of the data sets at Santa Fe Institute Time Series Prediction Competition (A.dat) [16]. It is discussed that this time series can be modeled by three coupled nonlinear ordinary differential equations and indicated that the structure of the attractor is similar to the Lorenz attractor with a fractional correlation dimension slightly larger than 2.0.

The third example is the first differences of the monthly number of measles cases reported in New York City from 1928 to 1963, which are also famous as the data used for

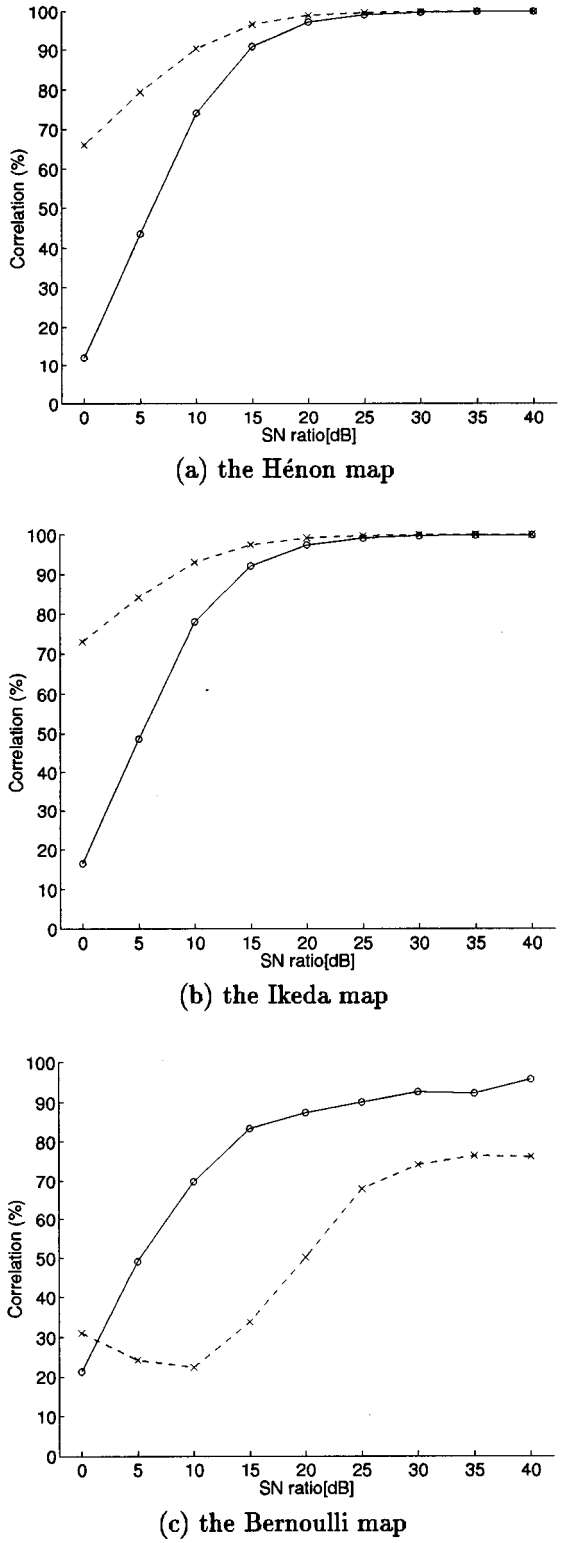

FIG. 6. Prediction performance evaluated on noisy dynamical systems of (a) the Hénon map, (b) the Ikeda map, and (c) the Bernoulli map. The abscissas show the levels of noise measured by the signal-to-noise ratio in decibels and the ordinates are correlation coefficients (%). In each figure, the solid lines with circles are for the conventional correlation coefficients and the dashed lines with crosses for the difference correlation coefficients. The number of time series is 2048. 100 initial conditions are prepared for each case and the averaged values are plotted.

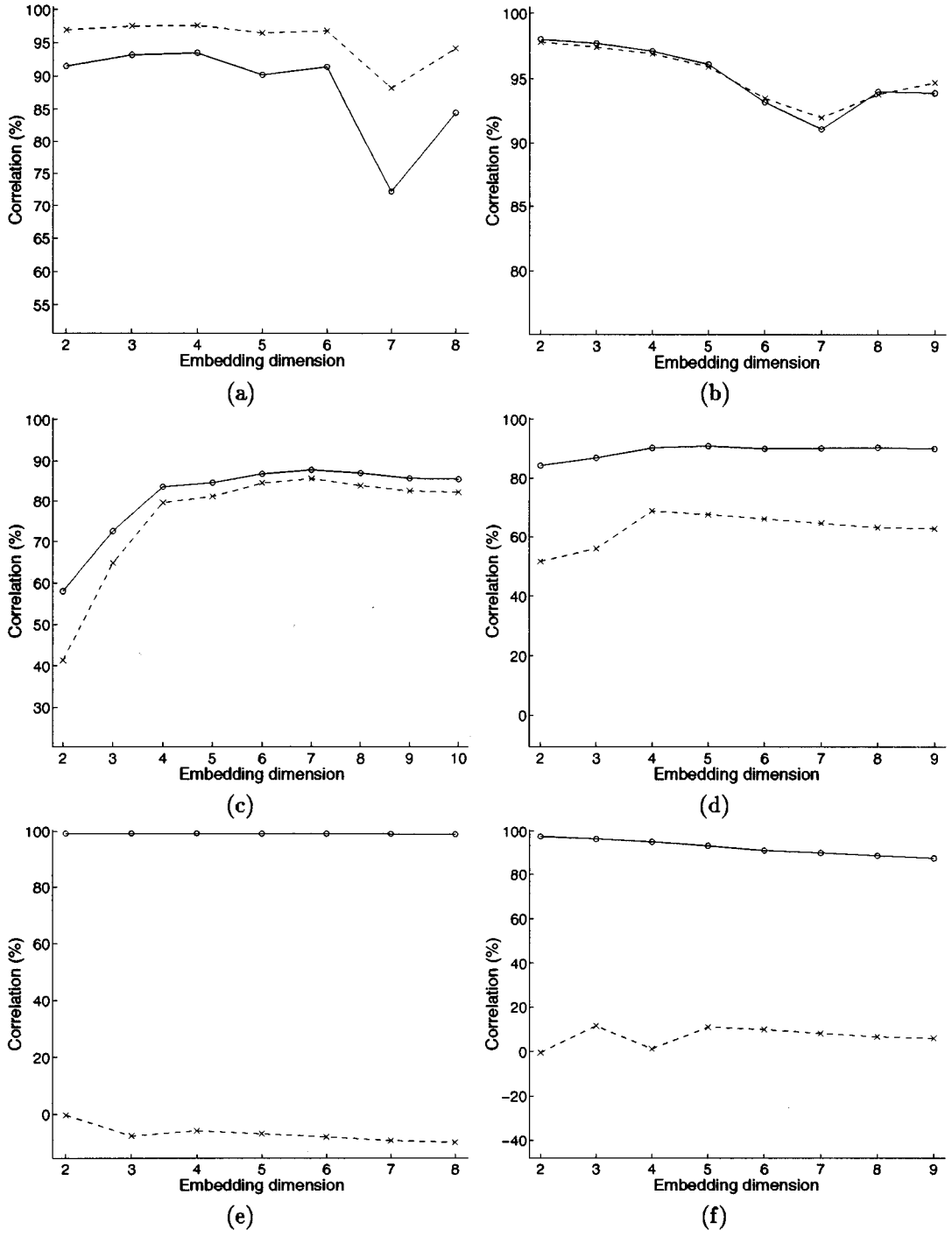

FIG. 7. Results of analyzing real time series from the natural world. (a) Squid axon response stimulated by periodic pulses, (b) Lorenz-like NH_3-FIR laser data (A.dat of Santa Fe Institute Prediction Competition), (c) measles data from Sugihara, (d) annual sunspot numbers, (e) New York index data, and (f) electroencephalographic (EEG) potentials from Rapp. Both conventional and difference correlation coefficients are calculated for the one-step-ahead prediction. Abscissas represent embedding dimensions and ordinates correlation coefficients. Solid lines with circles indicate the conventional correlation coefficients and dashed lines with crosses the difference correlation coefficients.

nonlinear forecasting analysis by Sugihara and May [3]. In Ref. [3] it is reported that the measles data are possibly described by a two- to three-dimensional chaotic attractor.

The fourth example is Wolfer's sunspot numbers, which have long been used as one of the standard time series since Yule [17]. This time series is annual time series recorded from 1700 to 1993.

The fifth and last examples are financial time series and electroencephalographic (EEG) potentials.

The financial time series is the New York index time series. Although many analyses have been applied on financial time series, it is considered that none of the tests are conclusive regarding the existence of low-dimensional chaos for complex behavior of financial time series.

The EEG time series has also been one of the most intensively analyzed data from the viewpoints of nonlinear low-dimensional chaos. Although previous results on EEGs by a dimensional analysis suggested possible evidence of low-dimensional nonlinearity [18], recent reexaminations with surrogate data sets do not necessarily imply a nonlinear structure of low-dimensional chaos [19]. The analyzed EEG in this paper is the same as the one in Refs. [18,19]. This EEG is measured from the electrode of O_z [18].

Results by the proposed algorithm are shown in Fig. 7. In Fig. 7, the variations of the conventional and the difference correlation coefficients are shown with changing embedding dimensions. From these results, we can read the following tendencies.

The results shown in Figs. 7(a)–7(c) are very similar to those of typical nonlinear dynamical systems; not only the conventional correlation coefficients, but also the difference correlation coefficients take high values. It is worth noting here that these results are in good agreement with those obtained in previous analyses, namely, these time series are considered to be low-dimensional chaos [13–16,3].

For the annual sunspot numbers, it is seen that the conventional correlation coefficients are relatively high values, but the difference correlation coefficients are low. Although the results shown here are only those obtained for the one-step-ahead prediction, it is hard to say whether or not the annual sunspot numbers are similar to those of typical dynamical systems.

For the financial time series and EEG data, it is clearly seen that the results with the difference correlation coefficients are significantly different from those of model dynamical systems, but they are similar to that of colored noise. While the conventional correlation coefficients are very high values in any reconstructing dimensions, the difference correlation coefficients are very low. From these results, we can say that there is less of a possibility that these time series are produced from low-dimensional nonlinear dynamical systems.

V. CONCLUSION

We have applied a nonlinear prediction algorithm to time series data, produced from both deterministic chaos and colored noise with the power-law spectra or random fractal sequences. We have shown that the difference correlation coefficient or the correlation coefficient between first-difference time series obtained from actual time series and predicted time series can be a good discrimination statistic between deterministic chaos and colored noise with the $1/f^{\alpha}$ power spectrum.

We also analyze the limitation of distinguishing noisy chaos from colored noise and show that it is possible that even though deterministic chaos is corrupted by a relatively large amount of observational noise, the deterministic chaos can be distinguished from stochastic noise because the combination of discriminant statistics, the conventional correlation coefficients, and the difference correlation coefficients shows the different property and therefore can be a good criterion. It is important in the future to investigate this method from other view points, for example, how discriminant performance is affected by the length of time series or the resolution of data points, and to give a theoretical explanation.

ACKNOWLEDGMENTS

The authors would like to thank Professor Takeshi Matozaki (Science University of Tokyo) for his encouragement of this research, Professor Alistair I. Mees (University of Western Australia) for his fruitful discussions, Professor George Sugihara (University of California) for providing his measles data series, and Professor Paul E. Rapp (The Medical College of Pennsylvania) for his valuable comments and for providing EEG data sets. The research was partly supported by Grants-in-Aid for Scientific Research (C) (Grant No. 078321019) and on Priority Areas (Grant No. 08279103) from the Ministry of Education, Culture and Science of Japan.

[1] T. Ikeguchi and K. Aihara, Int. J. Bifurc. Chaos (to be published).
[2] T. Tanaka, K. Aihara, and M. Taki, Phys. Rev. E **54**, 2122 (1996).
[3] G. Sugihara and R. M. May, Nature **344**, 734 (1990).
[4] D. J. Wales, Nature **350**, 485 (1991).
[5] A. A. Tsonis and J. B. Elsner, Nature **358**, 217 (1992).
[6] T. Ikeguchi and K. Aihara, IEICE Trans. Fundamentals **E78-A**, 1291 (1995).
[7] M. Hénon, Commun. Math. Phys. **50**, 69 (1976).
[8] K. Ikeda, Opt. Commun. **30**, 257 (1979).
[9] Y. Aizawa and T. Kohyama, Prog. Theor. Phys. **71**, 847 (1984).
[10] J. Theiler, Phys. Lett. A **133**, 195 (1988).
[11] A. R. Osborne and A. Provenzale, Physica D (Utrecht) **35**, 357 (1989).
[12] E. N. Lorenz, J. Atomos. Sci. **26**, 636 (1969).
[13] G. Matsumoto, K. Aihara, Y. Hanyu, N. Takahashi, S. Yoshizawa, and Jinichi Nagumo, Phys. Lett. A **123**, 162 (1987).
[14] N. Takahasi, Y. Hanyu, T. Musha, R. Kubo, and G. Matsumoto, Physica D (Utrecht) **43**, 318 (1990).
[15] A. Mees *et al.*, Phys. Lett. A **169**, 41 (1992).
[16] *Time Series Prediction: Forecasting the Future and Understanding the Past*, edited by A. S. Weigend and N. A. Gershenfeld (Addison-Wesley, Reading, MA, 1993).
[17] G. U. Yule, Philos. Trans. R. Soc. London Ser. A **226**, 267 (1927).
[18] P. E. Rapp *et al.*, Brain Topogr. **2**, 99 (1989).
[19] J. Theiler and P. E. Rapp, Electroencephalogr. Clin. Neurophysiol. **98**, 213 (1996).